Published in final edited form as:
Circulation. 2009 March 3; 119(8): 1124–1134. doi:10.1161/CIRCULATIONAHA.108.812537.

Ligand-activated PPAR-γ protects against ischemic cerebral infarction and neuronal apoptosis by 14-3-3ε upregulation

Jui-Sheng Wu, M.S.[1,2], **Wai-Mui Cheung, B.S.**[1], **Yau-Sheng Tsai, Ph.D.**[3], **Yi-Tong Chen, B.S.**[1], **Wen-Hsuan Fong, M.S.**[1], **Hsin-Da Tsai, M.S.**[1], **Yu-Chang Chen, M.S.**[1], **Jun-Yang Liou, Ph.D.**[4], **Song-Kun Shyue, Ph.D.**[1], **Jin-Jer Chen, M.D.**[1], **Y. Eugene Chen, M.D., Ph.D.**[5], **Nobuyo Maeda, Ph.D.**[6], **Kenneth K. Wu, M.D., Ph.D.**[4,7,§], and **Teng-Nan Lin, Ph.D.**[1,§]

[1]Institute of Biomedical Sciences, Academia Sinica, Taipei, Taiwan

[2]Graduate Institute of Life Sciences, National Defense Medical Center; Taipei, Taiwan

[3]Graduate Institute of Clinical Medicine, National Cheng Kung University Medical College, Tainan, Taiwan

[4]National Health Research Institutes, Zhunan, Taiwan

[5]Cardiovascular Center, University of Michigan Medical Center, Ann Arbor, Michigan, USA

[6]Department of Pathology and Laboratory Medicine, University of North Carolina, Chapel Hill, North Carolina, USA

[7]University of Texas Health Science Center in Houston, Houston, Texas USA

Abstract

Background—Thiazolidinediones (TZD) were reported to protect against ischemia-reperfusion (I/R) injury. Their protective actions are considered to be PPAR-γ (peroxisome proliferator-activated receptor γ)-dependent. However, it is unclear how PPAR-γ activation confers resistance to I/R.

Methods and Results—We evaluated the effects of rosiglitazone or PPAR-γ overexpression on cerebral infarction in a rat model and investigated the anti-apoptotic actions in N2-A neuroblastoma cell model. Rosiglitazone or PPAR-γ overexpression significantly reduced infarct volume. The protective effect was abrogated by PPAR-γ siRNA. In mice with knockin of a PPAR-γ domain negative mutant, infarct volume was enhanced. Proteomic analysis reveals that brain 14-3-3ε was highly upregulated in rats treated with rosiglitazone. 14-3-3ε upregulation was abrogated by PPAR-γ siRNA or antagonist. Promoter analysis and chromatin immunoprecipitation reveal that rosiglitazone induced PPAR-γ binding to specific regulatory elements on 14-3-3ε promoter and thereby increased 14-3-3ε transcription. 14-3-3ε siRNA abrogated the anti-apoptotic actions of rosiglitazone or PPAR-γ overexpression while 14-3-3ε recombinant proteins rescued

[§]**Address correspondence to**: Kenneth K. Wu, MD, PhD, National Health Research Institutes, Zhunan Township, Miaoli County 350, Taiwan. Fax: 886-37-586402, kkgo@nhri.org.tw and Teng-nan Lin, PhD, Institute of Biomedical Sciences, Academia Sinica, Taipei 11529, Taiwan. FAX: 886-2-2785-8847, bmltn@ibms.sinica.edu.tw.

Disclosure
None.

brain tissues and N2-A cells from ischemia-induced damage and apoptosis. Elevated 14-3-3ε enhanced binding of phosphorylated Bad, and protected mitochondrial membrane potential.

Conclusions—Ligand-activated PPAR-γ confers resistance to neuronal apoptosis and cerebral infarction by driving 14-3-3ε transcription. 14-3-3ε upregulation enhances sequestration of phosphorylated Bad and thereby suppresses apoptosis.

Keywords

Apoptosis; Infarction; Stroke; PPAR; 14-3-3ε

Introduction

Peroxisome proliferator-activated receptor-γ (PPAR-γ), a member of the PPAR nuclear receptor family, is a ligand-activated transcription factor that regulates diverse biological activities and plays major roles in important human diseases such as diabetes, metabolic syndrome and atherosclerosis (1). Several classes of PPAR-γ ligands have been identified. Naturally occurring fatty acid derivatives such as 15 deoxy-$\Delta^{12,14}$ prostaglandin J_2 (15d-PGJ_2) binds and activates PPAR-γ and is thought to mediate the anti-inflammatory action of PPAR-γ (2, 3). Synthetic PPAR-γ ligands such as thiazolidinedione (TZD) are clinically efficacious in treating type 2 diabetes (4). Ligand-activated PPAR-γ forms heterodimers with retinoid X receptor which binds PPAR response elements (PPRE) situated at the promoter region of target genes and regulates the gene expression (1). Extensive investigations have reported that ligand-activated PPAR-γ suppresses pro-inflammatory genes at the transcriptional level (5-8). The anti-inflammatory action of PPAR-γ ligands was considered to contribute to tissue protection. Rosiglitazone was reported to protect against ischemia-reperfusion (I/R) induced myocardial damage while troglitazone and pioglitazone protect against cerebral infarction in a rat I/R stroke model (9-11). We have previously reported that 15d-PGJ_2 was effective in reducing cerebral infarct volume in a rat model (12). Our previous *in vitro* data suggest that 15d-PGJ_2 and TZDs such as rosiglitazone protect neurons from oxidant-induced apoptosis (12). The purpose of this study was to evaluate the effects of rosiglitazone and PPAR-γ overexpression on neural apoptosis and to identify the downstream effector molecules. The results show that rosiglitazone and PPAR-γ overexpression protected against I/R damage in a rat stroke model and in mice with knockin of a PPAR-γ dominant negative mutant. Proteomic analysis of ischemic rat brain identified 14-3-3ε to be highly elevated in rosiglitazone-treated rats. Results from animal and cell experiments reveal that 14-3-3ε was upregulated by ligand-activated PPAR-γ at the transcriptional level. Knockdown of 14-3-3ε with RNAi abrogated the protective effect of rosiglitazone and PPAR-γ while ectopic expression of 14-3-3ε or infusion of 14-3-3ε proteins rescued brains from infarction and neuronal cells from ischemic damage.

Methods

Animal Models

The rat focal cerebral ischemia-reperfusion model was described previously (13, 14) (see supplemental materials). The PPAR-γ P465L mutant mice were prepared as previously

described (15). In brief, the inbred foundation colony was maintained by breeding heterozygous P465L mutant mice with inbred 129/SvEv mice. The production colony for experiments was maintained by breeding heterozygous P465L knockin mice on the 129/SvEv genetic background with C57BL/6J mice. This produced both wild type and heterozygous P465L knockin mice on the same inbred genetic background (129/SvEv X C57BL/6J F1). Littermate wild type serves as control mice.

Oxygen-glucose deprivation (OGD) cell model

Murine N2-A neuroblastoma cells (American Type Culture Collection) grown to 70% confluence were treated with rosiglitazone (Cayman) alone or in combination with GW9662, washed with deoxygenated glucose-free Hanks' balanced salt solution, and transferred to an anaerobic chamber (Model 1025, Forma Scientific) containing a gas mixture of 5% CO_2, 10% H_2, 85% N_2, and 0.02% to 0.1% O_2 (16, 17) for 3 h. After OGD, N2-A cells were cultured in glucose-containing Hanks' balanced salt solution under the normoxic condition in a 5% CO_2 incubator for various time periods.

Transient transfection

Mouse PPAR-γ1 expression plasmid was prepared by cloning PPAR-γ1 into pcDNA3.1+ vector. Specific PPAR-γ small interfering RNA (siRNA) and scrambled RNA (scRNA) were purchased from Ambion. 14-3-3ε expression plasmid was prepared as previously described (18). In brief, the complete coding sequence of 14-3-3ε was amplified by PCR and cloned into pcDNA3.1+ vector (Invitrogen). Specific 14-3-3ε siRNA was purchased from Santa Cruz. Lipofectamine 2000 (Invitrogen) was used as a transfection carrier according to manufacturer's instructions (see supplemental materials).

Reporter Assay

PPRE-reporter construct, acyl-CoA oxidase (ACO)-Luc, was prepared by cloning luciferase into an ACO vector, which contains 4 PPAR response elements (PPREs) and a minimal cytomegalovirus promoter. pCMV-β-galactosidase (β-Gal) plasmid was used as an internal control of transfection. For cloning 14-3-3ε promoter, a 1.6-kb (–1625 to +24) 5'-flanking region of human genomic sequence was amplified by PCR and cloned into pGL3 luciferase reporter (18). Transfection was performed as previously described (18) and described in supplemental materials.

Western Blot and Immunoprecipitation Analysis

Analysis of proteins in the cortex and N2-A cells by Western blotting was performed as described previously (12). Immunoprecipitation was performed as described (18). (See supplemental materials.)

Flow Cytometry

Flow cytometry was employed to analyze apoptosis and mitochondria membrane potential (see supplemental materials).

Intraventricular Injection of rosiglitazone, GW9662, PPAR-γ siRNA and 14-3-3ε siRNA

The procedure was performed as previously described (12). Briefly, anesthetized rats were placed in a stereotaxic apparatus; 50 ng (0.14 nmol) rosiglitazone, 165 ng (0.58 nmol) GW9662 or 0.1-2 nmol siRNA in 10 μL volume were injected into the right lateral ventricle at 2 μL/min at the following coordinates: Anterior, 2.5 mm caudal to bregma; Right, 2.8 mm lateral to midline; and Ventral, 3.0 mm ventral to dural surface. Periodic confirmation of proper placement of the needle was performed with infusionof fast green. Rosiglitazone, PPARγ siRNA or control was injected into the lateral ventricle for 24 h immediately after the 30 min transient occlusion. The extent of PPAR-γ knockdown by siRNA was quantified by RT-PCR at 24 h after reperfusion.

Intraventricular Infusion of PPAR-γ and 14-3-3ε recombinant proteins

Rats were anesthetized with chloral hydrate (360 mg/kg, i.p.). The brain infusion cannula was inserted into the right ventricle of the brain at a point located 2 mm lateral and 2 mm posterior to the bregma, and at a depth of 3 mm from the cortical surface. The osmotic pump (Alzet 1007D) with brain infusion kit ‖ was installed in subcutaneous pocket on the lateral back of the rats. An instant adhesive gel (Loctite 454) was used to affix the infusion cannula to the skull, and wound was closed with sutures. Recombinant PPAR-γ (Cayman), His-tagged 14-3-3ε (Cayman) or vehicle was infused continuously for 72 h (1.2 μg/day at a rate of 0.5 μL/h) via the osmotic pump prior to I/R.

RNA isolation, reverse transcription (RT) and polymerase chain reaction (PCR)

Total RNA isolation and RT-PCR amplication were performed as previously described (12) (see supplemental materials).

Two-dimensional gel electrophoresis (2-DGE) and mass spectrometry

Rat brain was homogenized and 130 μg of the supernatant proteins were subjected to 2-DGE analysis (see supplemental materials). Gels were stained and analyzed by ImageMaster 2-D analysis software. The gel images were normalized according to the total quantity in the analysis set. An expression intensity ratio larger than 2.0 was considered to be a significant change. Spots with significant changes were removed and analyzed by liquid chromatography and tandem mass spectrometry (LC-MS/MS) (see supplemental materials).

Chromatin Immunoprecipitation (ChIP) assay

ChIP assay was performed as previously described (18,19) (see supplemental materials).

Statistical Analysis

Analysis of variance (ANOVA) was used to compare the expression of proteins or infarct volumes. The level of significance for differences between groups was further analyzed with post-hoc Fisher's protected *t* tests by GB-STAT 5.0.4 (Dynamic Microsystem, Inc, Silver Springs, Md). $P<0.05$ was considered significant.

Statement of Responsibility

The authors had full access to and take full responsibility for the integrity of the data. All authors have read and agree to the manuscript as written.

Results

Rosiglitazone-PPAR-γ protects brain against I/R injury in a rat model

To evaluate the *in vivo* neuroprotective effect, rosiglitazone was injected intraventricularly immediately after 30-min ischemia and the infarct volume at the ipsilateral brain was measured 24 h later. There was no significant difference in physiologic variables between vehicle control and rosiglitazone-treated groups (supplemental Table S1). Rosiglitazone at 0.5 to 150 ng significantly reduced the infarct volume. The maximal reduction occurred at 50 ng while at higher concentrations (300 & 500 ng) it no longer had protective effect (Fig. 1a). We used 50 ng of rosiglitazone in the remaining studies. Infusion of rosiglitazone 2 h after reperfusion was still effective in reducing infarct volume (Fig. 1b). The protective effect of rosiglitazone was blocked by GW9662 (Fig. 1c). Intraventricular injection of a PPAR-γ siRNA for 24 h suppressed PPAR-γ mRNA in normal brain tissues (Fig. S1) as well as in ischemic brain tissues when compared to scRNA injection (Fig. 1d). The PPAR-γ siRNA injection immediately after the 30-min ischemia concentration-dependently abrogated the protective effect of rosiglitazone while scRNA had no effect (Fig. 1e). Intraventricular infusion of PPAR-γ proteins (5μg) for 72 h before I/R reduced the infarct volume by > 60% when compared to control (Fig. 1f). The essential role of PPAR-γ was further evaluated in mice with heterozygous knockin of a PPAR-γ dominant negative mutant, P465L (L/+). Wild-type or L/+ mice were subjected to 30 min ischemia followed by 24 h reperfusion. Compared to wild-type mice with a mean infarct volume of 8 mm^3, the infarct volume in L/+ mice was increased by about 80% (Fig. 1g).

The anti-apoptotic effect of rosiglitazone was evaluated in ischemic rat brain tissues. Rosiglitazone injection immediately after the 30-min ischemia reduced cleaved PARP and activated caspase 3 and caspase 9 when compared to vehicle (DMSO) (Fig. 2a). PPAR-γ siRNA abrogated the anti-apoptotic action of rosiglitazone (Fig. 2a), while infusion of recombinant PPAR-γ proteins suppressed the apoptotic changes (Fig. 2b). These results indicate that rosiglitazone protects brain from I/R-induced apoptosis.

Proteomic analysis identifies 14-3-3ε upregulation by rosiglitazone in ischemic brain

To identify proteins important in the rosiglitazone-PPAR-γ signaling pathway, we analyzed ischemic brain tissues by proteomics. Rats were subjected to a 30-min transient ischemia. Rosiglitazone or vehicle was administered right after ischemia for 24 h. Brain was isolated, homogenized and proteins were analyzed by 2-DGE. A spot with a very large increase in density in rosiglitazone vs. control (5.5-fold) was identified (Fig. 3a). The spot was removed and the protein identity was analyzed by LC-MS/MS. The protein matches 14-3-3ε. Western blot analysis confirmed that rosiglitazone pretreatment restored the suppressed 14-3-3ε proteins in ischemic brain tissues (Fig. 3b). To determine whether 14-3-3ε upregulation in brain tissues is PPAR-γ dependent, we analyzed 14-3-3ε proteins in the ipsilateral brain 24 h

after infusion of rosiglitazone or DMSO. Rosiglitazone increased 14-3-3ε proteins by >3 fold (Fig. 3c). This increase was inhibited by PPAR-γ siRNA. Infusion of recombinant PPAR-γ proteins also increased 14-3-3ε (Fig. 3d). Furthermore, 14-3-3ε proteins in L/+ mouse brain were reduced by ~50% when compared to wild-type brain (Fig. 3e).

Rosiglitazone upregulates 14-3-3ε transcription

To elucidate the mechanism by which 14-3-3ε expression is upregulated, we employed N2-A neuroblastoma cells as a model. Cells were incubated with rosiglitazone at increasing concentrations and 14-3-3ε proteins were analyzed 24 h later. Rosiglitazone concentration-dependently increased 14-3-3ε proteins (Fig. 4a). This increase was blocked by GW9662 (Fig. 4b) or PPAR-γ siRNA (Fig 4c). Transfection with PPAR-γ plasmids for 24 h increased 14-3-3ε proteins in a concentration-dependent manner (Fig. 4d).

We have previously cloned a ~1.6 kb 5'-flanking region of 14-3-3ε gene which harbors three PPRE between -1348 and -1625 (18). To determine the involvement of PPREs in rosiglitazone-induced 14-3-3ε upregulation, we transfected N2-A cells with this promoter fragment (p1625-LUC) or a 5'-deletion mutant in which the PPREs were removed (p1348-LUC). Rosiglitazone increased the p1625 promoter activity in a concentration-dependent manner (Fig. S2a), but did not increase p1348 activity (Fig. 4e). Overexpressoin of PPAR-γ by transient transfection of PPAR-γ plasmid (Fig. S2b) also increased the p1625 promoter activity (Fig. S2c) which was abrogated when the PPRE region was deleted (Fig. 4f). ChIP assays show that rosiglitazone induced binding of PPAR-γ but not PPAR-β/δ to PPRE-harboring region between -1554 and -1854 of 14-3-3ε promoter despite expressions of both PPAR proteins in this cell line (data not shown) (Fig. 4g). These results indicate that rosiglitazone selectively induced binding of PPAR-γ to 14-3-3ε PPREs, thereby activating 14-3-3ε promoter and upregulating 14-3-3ε protein expression.

14-3-3ε protects brain from I/R injury

To determine the role of 14-3-3ε upregulation in controlling I/R induced infarction, we infused rosiglitazone with 14-3-3ε siRNA or control scRNA immediately after the 30-min ischemia. Reduction of the infarct volume by rosiglitazone was abrogated by 14-3-3ε siRNA in a concentration-dependent manner (Fig. 5a). 14-3-3ε mRNA in siRNA treated brain was reduced when compared to scRNA control (Fig. 5a, inset). Conversely, overexpression of 14-3-3ε (Fig. 5b, inset) by infusion of recombinant 14-3-3ε proteins for 72 h before I/R reduced infarct volume in a dose-dependent fashion (Fig. 5b).

Rosiglitazone prevents neuronal apoptosis via PPAR-γ to 14-3-3ε pathway

To confirm that ligand-activated PPAR-γ prevents neuronal apoptosis via 14-3-3ε upregulation, N2-A cells were subjected to OGD for 3 h followed by reoxygenation for 24 h (H3R24) and cells with apoptosis were analyzed by flow cytometry. OGD (H3R24) increased percentage of apoptotic cells which was reduced by pretreatment with rosiglitazone (Fig. 6a). The effect of rosiglitazone was abrogated by GW9662 (Fig. 6a). OGD enhanced PARP cleavage and caspase 3 and 9 activation which were suppressed by rosiglitazone and reversed by GW9662 (Fig. 6b). To ascertain the anti-apoptotic action of ligand-activated PPAR-γ, we transfected N2-A with PPAR-γ siRNA and analyzed apoptotic

changes. PPAR-γ in N2-A cells was functional as evidenced by activation by rosiglitazone of a PPAR promoter construct, ACO-$(PPRE)_4$-Luc which was inhibited by GW9662 (Fig. S3a). PPAR-γ siRNA which suppressed PPAR-γ proteins (Fig. S3b) and mRNA (Fig. S3c) abrogated the ACO-$(PPRE)_4$ promoter activity induced by rosiglitazone (Fig. S3d). The anti-apoptotic effect of rosiglitazone was abrogated by PPAR-γ siRNA but not scRNA (Fig. 6c). Treatment of N2-A with PPAR-γ vectors reduced apoptotic cells (Fig. 6d). The results are consistent with inhibition of apoptosis by rosiglitazone via PPAR-γ.

To confirm that the neuroprotective effect of rosiglitazone and PPAR-γ overexpression is mediated by 14-3-3ε, we evaluated the effect of rosiglitazone on 14-3-3ε levels in OGD-injured N2-A. 14-3-3ε proteins were detected in N2-A which was enhanced by rosiglitazone (Fig. 7a). 14-3-3ε proteins were suppressed in OGD -treated cells which were restored by rosiglitazone but the rescue was prevented by GW9662 (Fig. 7a). Similarly, restoration of 14-3-3ε proteins under OGD insults was abrogated by PPAR-γ siRNA but not scRNA (Fig. 7b). Conversely, reduction of 14-3-3ε proteins in OGD-treated cells was attenuated by PPAR-γ transfection (Fig. 7c). These results suggest that rosiglitazone or PPAR-γ overexpression prevents 14-3-3ε suppression by OGD insults.

To determine if 14-3-3ε upregulation is essential for the anti-apoptotic action of rosiglitazone and PPAR-γ, we treated cells with rosiglitazone in the presence of 14-3-3ε siRNA or control scRNA and subjected them to OGD (H3R24). 14-3-3ε siRNA concentration-dependently suppressed 14-3-3ε proteins in N2-A (Fig. S4a). The anti-apoptotic effect of rosiglitazone and PPAR-γ overexpression was abrogated by 14-3-3ε siRNA but not scRNA (Fig. 7d and 7e). We next determined if 14-3-3ε overexpression rescues cells from OGD-induced apoptosis. 14-3-3ε overexpression by transient transfection (Fig. S4b) significantly reduced OGD-induced apoptotic cells (Fig. 7f).

Ligand-activated PPAR-γ restores phosphorylated Bad and its interaction with 14-3-3ε

The anti-apoptotic action of 14-3-3ε is attributed to binding and sequestering phosphorylated Bad (p-Bad). To understand how rosiglitazone-PPAR-γ protects against apoptosis via 14-3-3ε, we analyzed p-Bad under OGD stress and determined 14-3-3ε and p-Bad interaction. p-Bad was detected in control cells which was suppressed by OGD (H3R24) but was restored partially by rosiglitazone (Fig. 8a). Decline of p-Bad in OGD-treated cells correlates with that of 14-3-3ε and rosiglitazone restored both proteins in a correlative fashion (Fig. 8a). Decline of 14-3-3ε and p-Bad by OGD was attenuated by PPAR-γ overexpression (Fig. 8b). To determine whether rosiglitazone enhances binding of Bad by 14-3-3ε, we prepared cell lysates of OGD-injured N2-A treated with or without rosiglitazone. The lysate proteins were immunoprecipitated with a 14-3-3ε antibody and analyzed by Western blotting. In the presence of rosiglitazone, a large quantity of p-Bad and 14-3-3ε proteins were detected in the immunoprecipitate (Fig. 8c) consistent with enhanced binding of p-Bad to 14-3-3ε by rosiglitazone. To determine whether rosiglitazone and PPAR-γ attenuate Bad-induced mitochondrial damage, we measured mitochondrial membrane potential (MMP) by flow cytometry using JC-1 fluorescent probe. OGD (H3R12) caused a significant reduction of normal MMP cells which was attenuated by rosiglitazone (Fig. 8d) or PPAR-γ overexpression (Fig. 8e). The protective action of either treatment was

abrogated by 14-3-3ε siRNA and not control scRNA (Fig. 8d & 8e). Furthermore, 14-3-3ε overexpression attenuated OGD (H3R12)-induced MMP disruption (Fig. 8f).

Discussion

In this study, we identify a novel transcriptional mechanism by which TZDs such as rosiglitazone protect against ischemic neuronal apoptosis and cerebral infarction. Our results provide strong evidence for an essential role of PPAR-γ-mediated 14-3-3ε upregulation in neural protection. Suppression of PPAR-γ with RNAi or inhibition of PPAR-γ with pharmacological inhibitors abrogates the protective action of rosiglitazone *in vivo* and *in vitro*. Furthermore, PPAR-γ transfection or infusion of PPAR-γ proteins alone attenuates neuronal apoptosis and infarct volume in rats while knockin of a PPAR-γ mutant (P465L) aggravates infarction in mice. These results suggest that PPAR-γ activated by exogenous ligands such as rosiglitazone or certain endogenous ligands plays an essential role in protection against ischemic and hypoxic insults. Our data provide strong evidence for direct activation of 14-3-3ε transcription by PPAR-γ. We show that PPAR-γ binds to PPRE-harboring region of 14-3-3ε promoter and upregulates 14-3-3ε expression. Importantly, rosiglitazone restores 14-3-3ε expression in hypoxia-injured cells or brain tissues. Reduction of 14-3-3ε expression was recently detected by proteomic analysis in neonatal rat hypoxia/ischemia (20) but to our knowledge has not been reported in ischemic stroke. As reduction of 14-3-3ε makes the neural tissues vulnerable to damage, restoration of 14-3-3ε by rosiglitaznoe contributes to its protective action. The effect of rosiglitazone on 14-3-3ε restoration is PPAR-γ dependent. These results indicate that ligand-activated PPAR-γ drives 14-3-3ε expression and increases cellular 14-3-3ε proteins in normal and ischemic tissues. Our results further show that the protective actions of rosiglitazone or PPAR-γ overexpression depend on 14-3-3ε upregulation. Knockdown of 14-3-3ε renders rosiglitazone or PPAR-γ ineffective in protecting neural tissues whereas 14-3-3ε overexpression renders cells resistant to apoptosis. Furthermore, direct intraventricular injection of 14-3-3ε or PPAR-γ proteins attenuates the I/R-induced infarction in a dose-dependent manner. Intraventricular injection of growth factors, antibodies or inhibitory peptides was previously shown to control ischemic brain lesions (21,22). It is unclear how the injected proteins or peptides work. It was proposed that they may enter cells via endocytosis. Taken together, the results indicate that PPAR-γ mediated 14-3-3ε upregulation plays a crucial role in protection against neuronal apoptosis and cerebral infarction. This transcriptional pathway represents a new paradigm of cell and tissue protection.

Recent reports from our laboratory indicate that PPAR-δ ligands protect endothelial cells and colon cancer cells from apoptosis by inducing PPAR-δ binding to PPRE thereby enhancing 14-3-3ε proteins and increasing Bad sequestration (18,23). Promoter analysis reveals that ligand-activated PPAR-δ binds to the similar PPRE region as ligand-activated PPAR-γ (18). A C/EBP binding site was also implicated in PPAR-δ mediated 14-3-3ε expression (24). Thus, the protective actions of these two PPAR isoforms are mediated by a similar transcriptional mechanism. We provide evidence in this study that rosiglitazone selectively activates PPAR-γ-mediated 14-3-3ε upregulation. It does not induce PAPR-δ binding to the PPRE sites. It should be important to determine whether PPAR-δ ligands such as prostacyclin also selectively activate PPAR-δ-mediated 14-3-3ε upregulation. Another

important issue to be investigated is whether there exists cellular and tissue specificity for PPAR-γ vs. PPAR-δ mediated 14-3-3ε upregulation by their respective ligands. For example, it is unclear whether PPAR-γ ligands are capable of protecting endothelial cell survival via the PPAR-γ→14-3-3ε pathway, nor is it clear whether PPAR-δ ligands protect against I/R injury via PPAR-δ-mediated 14-3-3ε upregulation. Nevertheless, findings from this report together with results from previous reports suggest a potential synergistic interaction between PPAR-γ and PPAR-δ in cytoprotection via similar transcriptional activation of 14-3-3ε but depends on selective ligands.

14-3-3ε is a member of the 14-3-3 protein family (25), which bind diverse proteins and functions as a scaffold to facilitate or attenuate the activities of the binding proteins (26). Recently, 14-3-3 has been shown to co-localize with a variety of specific pathological deposits, such as neurofibrillary tangles, Pick bodies and Lewy bodies (27). Moreover, up-regulation of 14-3-3 immunoreactivity was noted in human brain infarction, which was considered to be involved in post-ischemic cell survival and astrogliosis (28,29). However, physiological functions or pathological roles of each given 14-3-3 isoform are generally unknown. In the present study, we identify the 14-3-3ε isoform as an important protector of brain. 14-3-3 has previously been shown to bind p-Bad, sequesters it in the cytoplasm and thereby prevents Bad-induced apoptosis via the mitochondrial pathway (30-32). We show in this study a quantitative correlation between 14-3-3ε proteins and p-Bad and an enhanced binding of p-Bad by PPAR-γ mediated 14-3-3ε upregulation. Furthermore, elevated 14-3-3ε contributes to normalization of MMP. Taken together, these results indicate that 14-3-3ε upregulation by ligand-activated PPAR-γ enhances p-Bad sequestration thereby reducing Bad translocation to mitochondria to disrupt MMP and induce apoptosis.

Rosiglitazone exerted a dose-related biphasic effect on infarct volume (Fig. 1a). The U-shaped dose response which was named hormesis has been noted with pharmacologically active compounds including corticosteroids and receptor agonists (33,34). The underlying mechanisms for biphasic actions are largely unknown. As we were interested in understanding how rosiglitazone protects I/R brain injury, we focused in this study on the concentrations that exert protective actions. It remains unclear why rosiglitazone at high doses (>300 ng) loses protective effect nor is it known whether at high doses, rosiglitazone is still active in PPAR-γ-dependent upregulation of 14-3-3ε expression. Further studies are needed to resolve this complex issue.

In summary, we have discovered a transcriptional pathway that is critical for protection against neuronal apoptosis and cerebral infarction. PPAR-γ-mediated 14-3-3ε upregulation represents an important transcription mechanism by which PPAR-γ agonists protect tissues from I/R injury and is a potential therapeutic target for important human diseases such as ischemic stroke and myocardial infarction.

Supplementary Material

Refer to Web version on PubMed Central for supplementary material.

Acknowledgments

The authors wish to thank the Core Facility Laboratory of Institute of Biomedical Sciences, Academia Sinica for technical assistance of LC-MS/MS analysis. We thank Dr. Chiun-Gung Juo for data consultation.

Sources of Funding

This study was supported by grants from National Science Council, Academia Sinica, National Health Research Institutes in Taiwan, and National Institutes of Health, USA (NS-23327 and HL-50675 to KKW; DK67320 to NM; HL-68878, HL-75397 and HL-89544 to YEC).

References

1. Semple RK, Chatterjee VK, O'Rahilly S. PPAR gamma and human metabolic disease. J. Clin. Invest. 2006; 116:581–589. [PubMed: 16511590]
2. Forman BM, Tontonoz P, Chen J, Brun RP, Spiegelman BM, Evans RM. 15-Deoxy-$\Delta^{12,14}$-Prostaglandin J_2 is a ligand for the adipocyte determination factor PPARγ. Cell. 1995; 83:803–812. [PubMed: 8521497]
3. Kliewer SA, Lenhard JM, Willson TM, Patel L, Morris DC, Lehmann JM. A prostaglandin J_2 metabolite binds peroxisome proliferator-activated receptor γ and promotes adipocyte differentiation. Cell. 1995; 83:813–819. [PubMed: 8521498]
4. Lehmann JM, Moore LB, Smith-Oliver TA, Wilkison WO, Willson TM, Kliewer SA. An antidiabetic thiazolidinedione is a high affinity ligand for peroxisome proliferator-activated receptor-γ (PPAR-γ). J. Biol. Chem. 1995; 270:12953–12956. [PubMed: 7768881]
5. Ricote M, Li AC, Willson TM, Kelly CJ, Glass CK. The peroxisome proliferator-activated receptor-γ is a negative regulator of macrophage activation. Nature. 1998; 391:79–82. [PubMed: 9422508]
6. Jiang C, Ting AT, Seed B. PPAR-γ agonists inhibit production of monocyte inflammatory cytokines. Nature. 1998; 391:82–86. [PubMed: 9422509]
7. Chawla A, Barak Y, Nagy L, Liao D, Tontonoz P, Evans RM. PPAR-γ dependent and independent effects on macrophage-gene expression in lipid metabolism and inflammation. Nature Med. 2001; 7:48–52. [PubMed: 11135615]
8. Welch JS, Ricote M, Akiyama TE, Gonzalez FJ, Glass CK. PPAR-γ and PPAR-δ negatively regulate specific subsets of lipopolysaccharide and IFN-γ target genes in macrophages. Proc. Natl. Acad. Sci. USA. 2003; 100:6712–6717. [PubMed: 12740443]
9. Yue TL, Chen J, Bao W, Narayanan PK, Bril A, Jiang W, Lysko PG, Gu JL, Boyce R, Zimmerman DM, Hart TK, Buckingham RE, Ohlstein EH. In vivo myocardial protection from ischemia/reperfusion injury by the peroxisome proliferator–activated receptor-γ agonist rosiglitazone. Circulation. 2001; 104:2588–2594. [PubMed: 11714655]
10. Shimazu T, Inoue I, Araki N, Asano Y, Sawada M, Furuya D, Nagoya H, Greenberg JH. A peroxisome proliferator-activated receptor-γ agonist reduces infarct size in transient but not in permanent ischemia. Stroke. 2005; 36:353–359. [PubMed: 15618443]
11. Sundararajan S, Gamboa JL, Victor NA, Wanderi EW, Lust WD, Landreth GE. Peroxisome proliferator-activated receptor-gamma ligands reduce inflammation and infarction size in transient focal ischemia. Neurosci. 2005; 130:685–96.
12. Lin TN, Cheung WM, Wu JS, Chen JJ, Lin H, Chen JJ, Liou JY, Shyue SK, Wu KK. 15d-Prostaglandin J_2 protects brain from ischemia-reperfusion injury. Athero. Thromb. Vasc. Biol. 2006; 26:481–487.
13. Chen ST, Hsu CY, Hogan EL, Macriq H, Balentine JD. A model of focal ischemic stroke in the rat: reproducible extensive cortical infarction. Stroke. 1986; 17:738–743. [PubMed: 2943059]
14. Lin TN, He YY, Wu G, Khan M, Hsu CY. Effect of brain edema on infarct volume in a focal cerebral ischemia model in the rat. Stroke. 1993; 24:117–121. [PubMed: 8418534]
15. Tsai YS, Kim HJ, Takahashi N, Kim HS, Hagaman JR, Kim JK, Maeda N. Hypertension and abnormal fat distribution but not insulin resistance in mice with P465L PPARgamma. J. Clin. Invest. 2004; 114:240–249. [PubMed: 15254591]

16. Goldberg MP, Choi DW. Combined oxygen and glucose deprivation in cortical cell culture: calcium-dependent and calcium-independent mechanisms of neuronal injury. J. Neurosci. 1993; 13:3510–3524. [PubMed: 8101871]

17. Hu CJ, Chen SD, Yang DI, Lin TN, Chen CM, Huang TH, Hsu CY. Promoter region methylation and reduced expression of thrombospondin-1 after oxygen-glucose deprivation in murine cerebral endothelial cells. J. Cereb. Blood Flow Metab. 2006; 26:1519–1526. [PubMed: 16570076]

18. Liou JY, Lee S, Ghelani D, Matijevic-Aleksic N, Wu KK. Protection of endothelial survival by peroxisome proliferator-activated receptor-δ mediated 14-3-3 upregulation. Athero. Thromb. Vasc. Biol. 2006; 26:1481–1487.

19. Deng WG, Zhu Y, Wu KK. Role of p300 and PCAF in regulating cyclooxygenase-2 promoter activation by inflammatory mediators. Blood. 2004; 103:2135–2142. [PubMed: 14630807]

20. Hu X, Rea HC, Wiktorowicz JE, Perez-Polo JR. Proteomic analysis of hypoxia/ischemia-induced alteration of cortical development and dopamine neurotransmission in neonatal rat. J. Proteome. Res. 2006; 5:2396–2404. [PubMed: 16944952]

21. Hara H, Friedlander RM, Gagliardini V, Ayata C, Fink K, Huang Z, Shimizu-Sasamata M, Yuan J, Moskowitz MA. Inhibition of interleukin 1beta converting enzyme family proteases reduces ischemic and excitotoxic neuronal damage. Proc. Natl. Acad. Sci. U. S. A. 1997; 94:2007–2012. [PubMed: 9050895]

22. Liu K, Mori S, Takahashi HK, Tomono Y, Wake H, Kanke T, Sato Y, Hiraga N, Adachi N, Yoshino T, Nishibori M. Anti-high mobility group box 1 monoclonal antibody ameliorates brain infarction induced by transient ischemia in rats. FASEB J. 2007; 21:3904–3916. [PubMed: 17628015]

23. Liou JY, Ghelani D, Yeh S, Wu KK. Nonsteroidal anti-inflammatory drugs induce colorectal cancer cell apoptosis by suppressing 14-3-3epsilon. Cancer Res. 2007; 67:3185–3191. [PubMed: 17409426]

24. Brunelli L, Cieslik KA, Alcorn JL, Vatta M, Baldini A. Peroxisome proliferator-activated receptor-delta upregulates 14-3-3 epsilon in human endothelial cells via CCAAT/enhancer binding protein-beta. Circ. Res. 2007; 100:e59–e71. [PubMed: 17303761]

25. Fu H, Subramanian RR, Masters SC. 14-3-3 proteins: structure, function, and regulation. Annu. Rev. Pharmacol. Toxicol. 2000; 40:617–647. [PubMed: 10836149]

26. Tzivion G, Avruch J. 14-3-3 proteins: active cofactors in cellular regulation by serine/threonine phosphorylation. J. Biol. Chem. 2002; 277:3061–3064. [PubMed: 11709560]

27. Aitken A. 14-3-3 proteins: a historic overview. Semin. Cancer Biol. 2006; 16:162–172. [PubMed: 16678438]

28. Kawamoto Y, Akiguchi I, Tomimoto H, Shirakashi Y, Honjo Y, Budka H. Upregulated expression of 14-3-3 proteins in astrocytes from human cerebrovascular ischemic lesions. Stroke. 2006; 37:830–835. [PubMed: 16424378]

29. Umahara T, Uchihara T, Tsuchiya K, Nakamura A, Iwamoto T. Intranuclear localization and isoform-dependent translocation of 14-3-3 proteins in human brain with infarction. J. Neurol. Sci. 2007; 260:159–166. [PubMed: 17561120]

30. Datta SR, Dudek H, Tao X, Masters S, Fu H, Gotoh Y, Greenberg ME. Akt phosphorylation of BAD couples survival signals to the cell-intrinsic death machinery. Cell. 1997; 91:231–241. [PubMed: 9346240]

31. Zha J, Harada H, Yang E, Jockel J, Korsmeyer SJ. Serine phosphorylation of death agonist BAD in response to survival factor results in binding to 14-3-3 Not BCL-X_L. Cell. 1996; 87:619–628. [PubMed: 8929531]

32. Zha J, Harada H, Osipov K, Jockel J, Waksman G, Korsmeyer SJ. BH3 domain of BAD is required for heterodimerization with BCL-X_L and pro-apoptotic activity. J. Biol. Chem. 1997; 272:24101–24104. [PubMed: 9305851]

33. Calabrese EJ, Baldwin LA. U-shaped dose-responses in biology, toxicology, and public health. Annu. Rev. Public Health. 2001; 22:15–33. [PubMed: 11274508]

34. Joels M. Corticosteroid effects in the brain: U-shape it. Trends Pharmacol. Sci. 2006; 27:244–250. [PubMed: 16584791]

Clinical Summary

Ischemia-reperfusion (I/R) injury is a major cause of cardiovascular diseases. The antidiabetic thiazolidinediones (TZD) were reported to protect against I/R injury. However, the mechanism of actions is unknown. We postulated that TZDs protect against I/R injury by driving peroxisome proliferatior-activated receptor-γ (PPAR-γ) mediated gene expression. To test this hypothesis, we evaluated the effect of rosiglitazone on infract volume in a rat cerebral I/R model. Rosiglitazone reduced infarct volume and suppressed neural apoptosis in a PPAR-γ dependent manner. Proteomic analysis revealed elevation of 14-3-3ε in rosiglitazone-treated brain tissues. 14-3-3ε upregulation was abrogated by PPAR-γ siRNA. Rosilgitazone and PPAR-γ overexpression (Rosi/PPAR-γ) increased 14-3-3ε promoter activities in a neuronal cell line N2-A. Rosiglitazone induced PPAR-γ but not PPAR-δ binding to PPAR response elements of 14-3-3ε promoter. 14-3-3ε upregulation plays a crucial role in conferring protection against I/R injury as knockdown of 14-3-3ε with siRNA abrogated the protective effect of Rosi/PPAR-γ while injection of 14-3-3ε expression vectors or recombinant proteins rescued tissues from I/R injury. 14-3-3ε upregulation was accompanied by increased binding and sequestration of phosphorylated Bad. These results indicate that rosiglitazone protects against I/R injury by activating PPAR-γ, thereby enhancing 14-3-3ε expression, increasing Bad sequestration and attenuating Bad-mediated apoptosis. Taken together with recent reports that prostacyclin inhibits apoptosis by activating PPAR-δ mediated 14-3-3ε upregulation in cultured endothelial cells, the results indicate that 14-3-3ε upregulation by ligand-restricted PPAR-γ or PPAR-δ activation represents a novel pathway for cytoprotection and a target for treating diseases such as ischemic stroke and myocardial infarction.

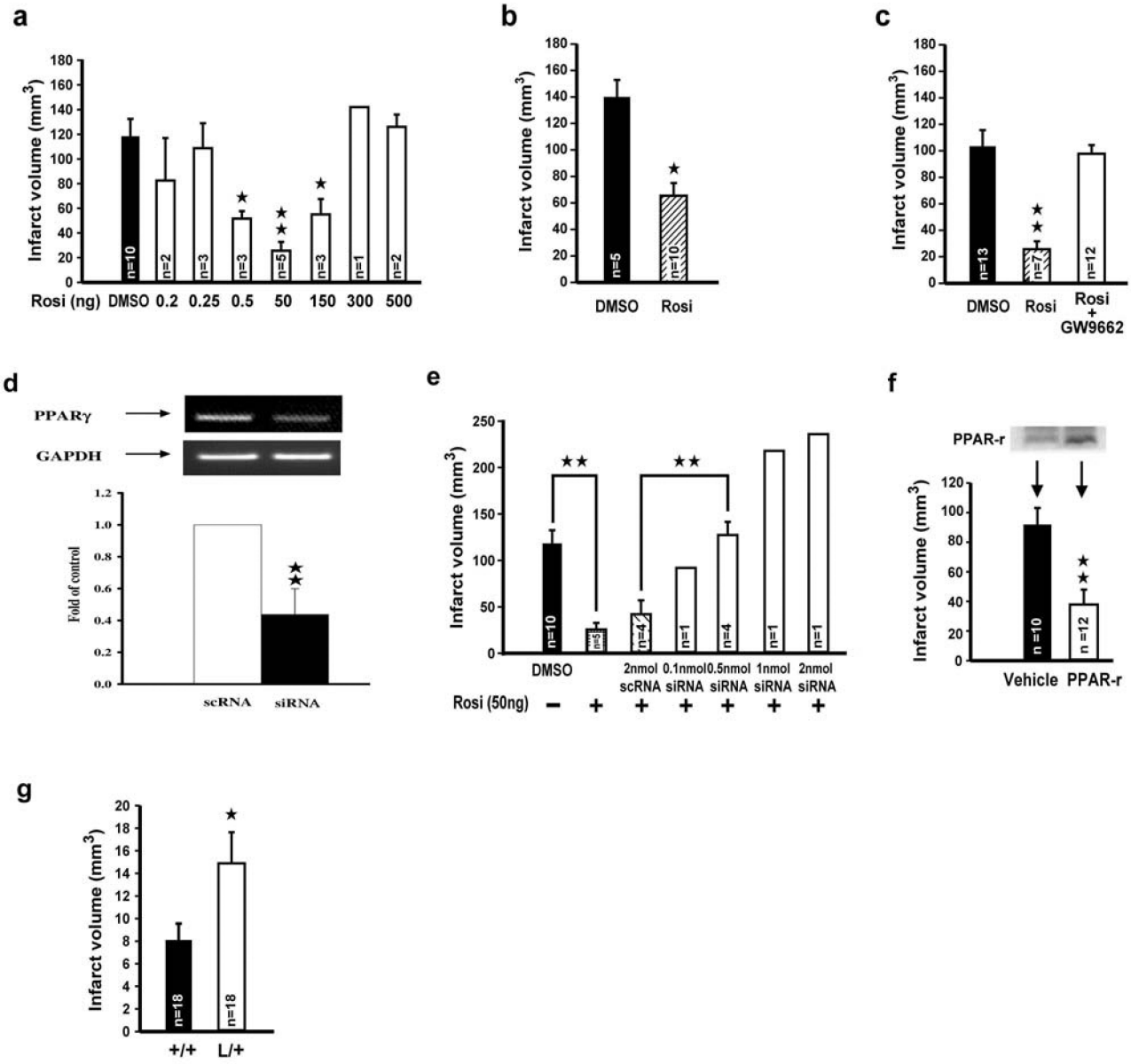

Figure 1. Rosiglitazone and PPAR-γ reduce ischemic brain injury *in vivo*

(a) Rosiglitazone was injected intraventricularly immediately after 30-min ischemia. Infarct volumes were determined after 24 h reperfusion. **(b)** Rosiglitazone (50 ng) was infused 2 h after a 30-min transient occlusion. **(c)** Rosiglitazone with & without GW9662 was infused. **(d)** PPAR-γ siRNA (0.5 nmol) or scRNA (2 nmol) was infused intraventricularly immediately after ischemia and PPAR-γ mRNA of brain tissues was measured 24 h later. The upper panel shows a representative gel and the lower panel, mean ± SD of densitometric analysis of four independent experiments. **(e)** Rosiglitazone with or without PPAR-γ siRNA was infused immediately after 30-min ischemia, and infarct volume was measured 24 h later. **(f)** Recombinant PPAR-γ protein (5 μg) was infused intraventricularly for 72 h before a 30-min ischemia. The inset indicates cortical PPAR-γ protein levels at 24 h after reperfusion. **(g)** PPAR-γ P465L dominant negative mutant mice (L/+) and wild type

littermate controls (+/+) were subjected to 30-min ischemia and 24 h reperfusoin. Each bar denotes mean ± SD (n as indicated). *P<0.05. **P<0.01.

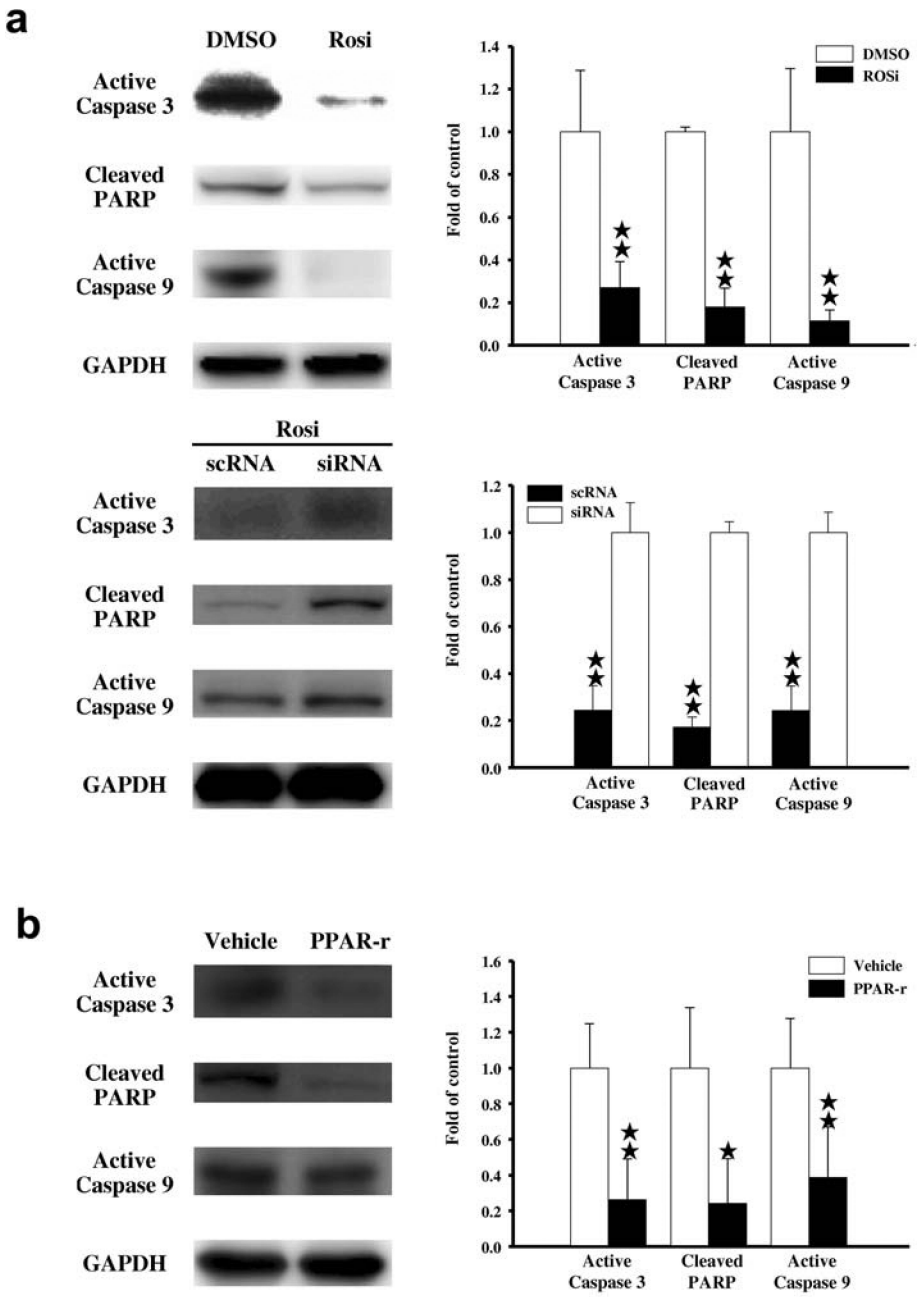

Figure 2. Analysis of apoptotic signals in ischemic brain

(a) Rosiglitazone (50 ng) or DMSO was injected with PPAR-γ siRNA or control scRNA, immediately after 30 min ischemia. Active caspases and cleaved PARP were analyzed by Western blotting. **(b)** Recombinant PPAR-γ proteins were infused for 72 h before I/R. Left panels show representative blots and right panels, densitometry of three experiments. **p*<0.05; ** *p*<0.01.

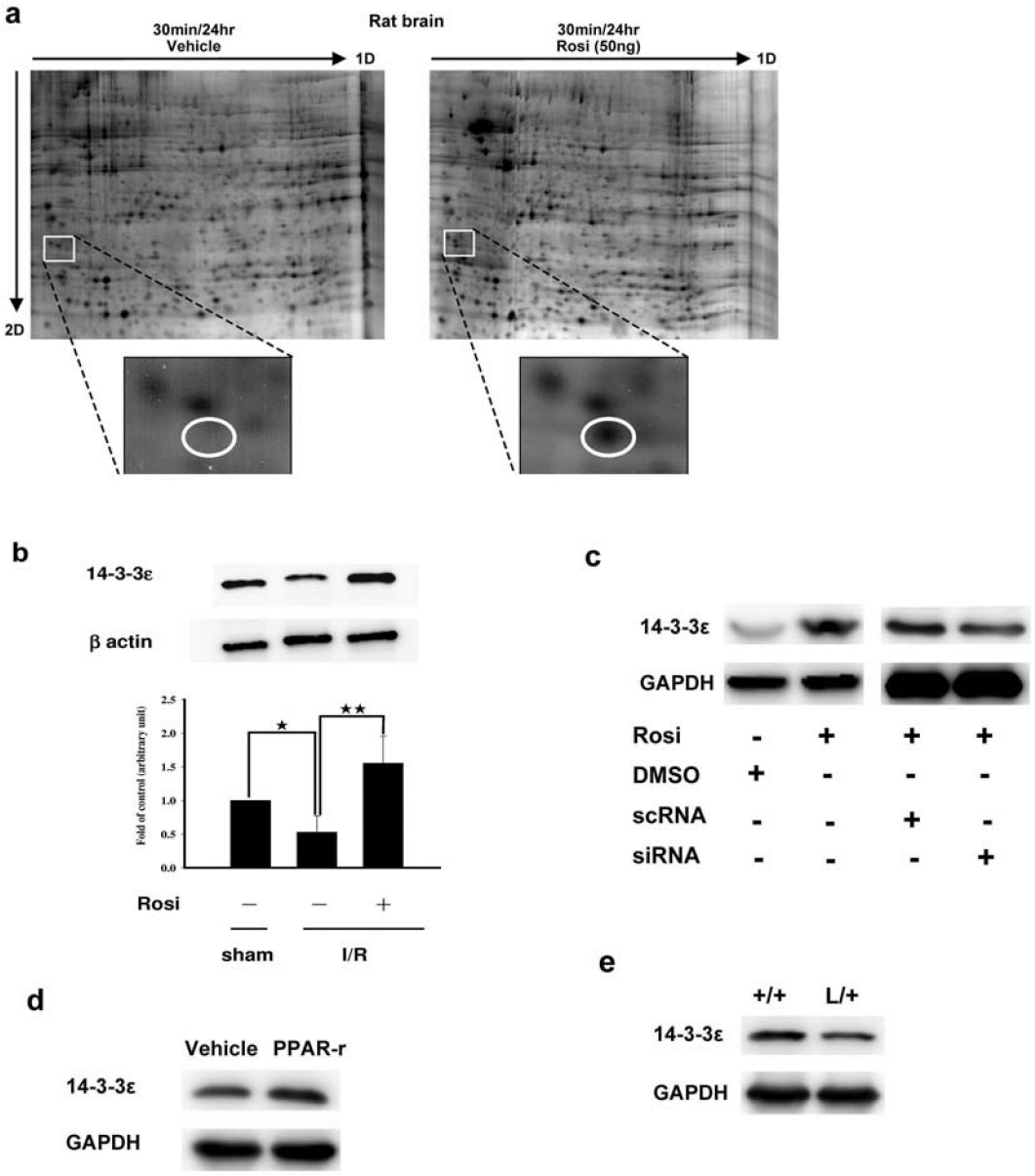

Figure 3. 14-3-3ε is increased in rosiglitazone-treated ischemic brain

(a) Rats were subjected to I/R with or without Rosi treatment. Proteins in rat brains were analyzed with 2-DGE. The insets show a spot with increased density in Rosi-treated vs. control brain. Analysis by LC-MS/MS identified this spot to be 14-3-3ε. Similar results were obtained in two other experiments. **(b)** Western blot analysis of 14-3-3ε in I/R vs. sham. Rats were treated with rosiglitazone or DMSO immediately after 30-min ischemia. Upper panel shows a representative blot and the lower panel the error bars from 3 independent experiments. Each bar denotes mean ± SD. *$p<0.05$, **$p<0.01$. **(c)** 14-3-3ε protein levels in brain tissues treated with or without rosiglitazone in the presence or absence of PPAR-γ siRNA or control scRNA. **(d)** 14-3-3ε proteins in brain tissues treated with recombinant PPAR-γ proteins or vehicle. **(e)** 14-3-3ε protein levels in wild-type (+/+) and L/+ mutant mouse brain tissues. Similar results were obtained in two other experiments.

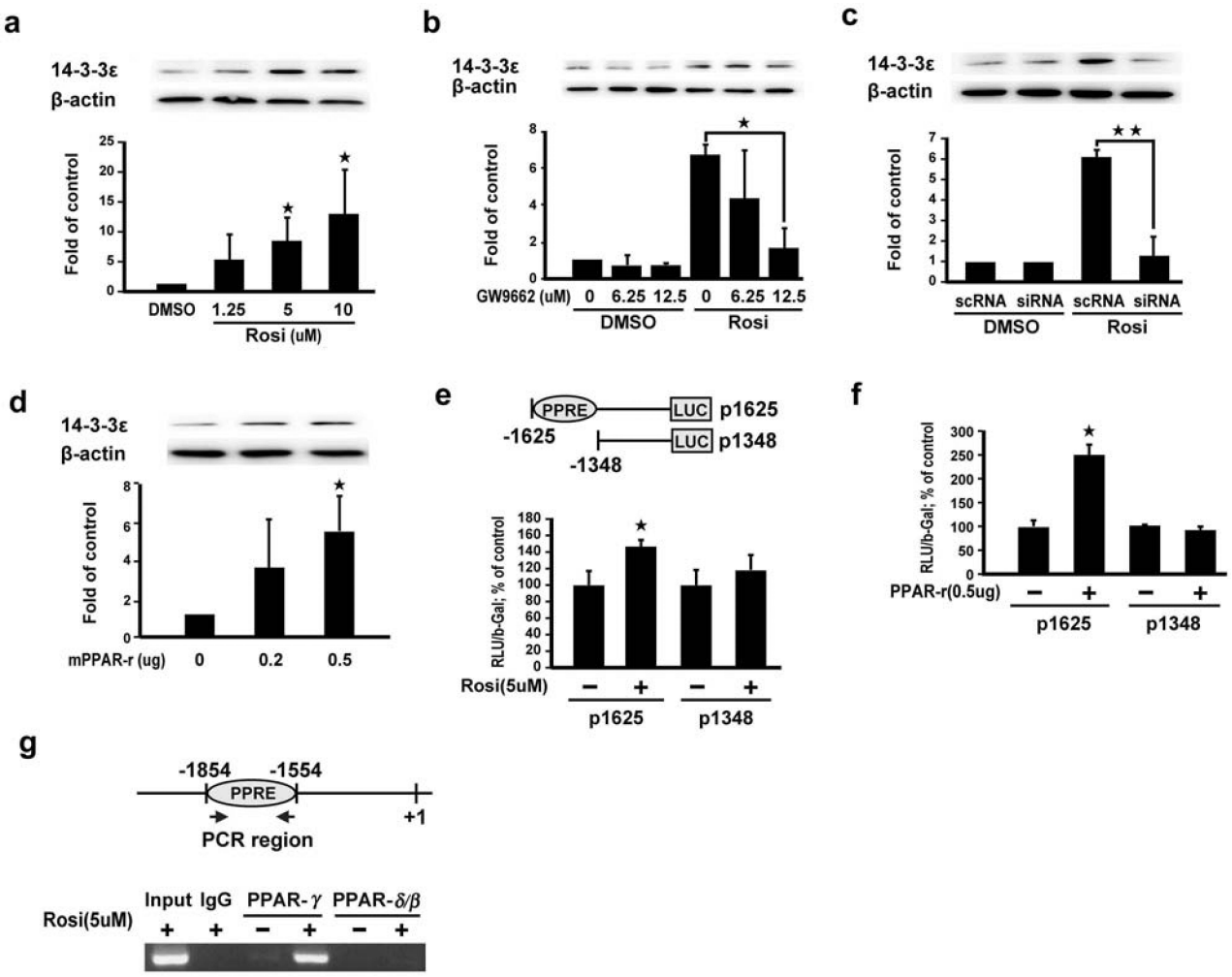

Figure 4. Ligand-activated PPAR-γ increases 14-3-3ε transcription

(a-d) 14-3-3ε proteins were analyzed by Western blotting in N2-A cells treated with rosiglitazone **(a)**, rosiglitazone in the presence of GW9662 **(b)**, rosiglitazone in the presence of PPAR-γ siRNA or scRNA **(c)**, or PPAR-γ expression vectors (mPPAR-γ) **(d)**. **(e) & (f)** N2-A cells transfected with 14-3-3ε promoter constructs p1625 or p1348 were treated with rosiglitazone **(e)** or PPAR-γ **(f)**. Promoter activity was expressed as relative light unit (RLU) using β-gal (b-Gal) as control to normalize the activity. **(g)** ChIP analysis of PPAR-γ binding to the PPRE region (upper panel) of 14-3-3ε promoter. Binding of PPAR-β/δ was included as a control. Each bar represents mean ± SD of at least three independent experiments conducted in triplicate. *P<0.05. **P<0.01.

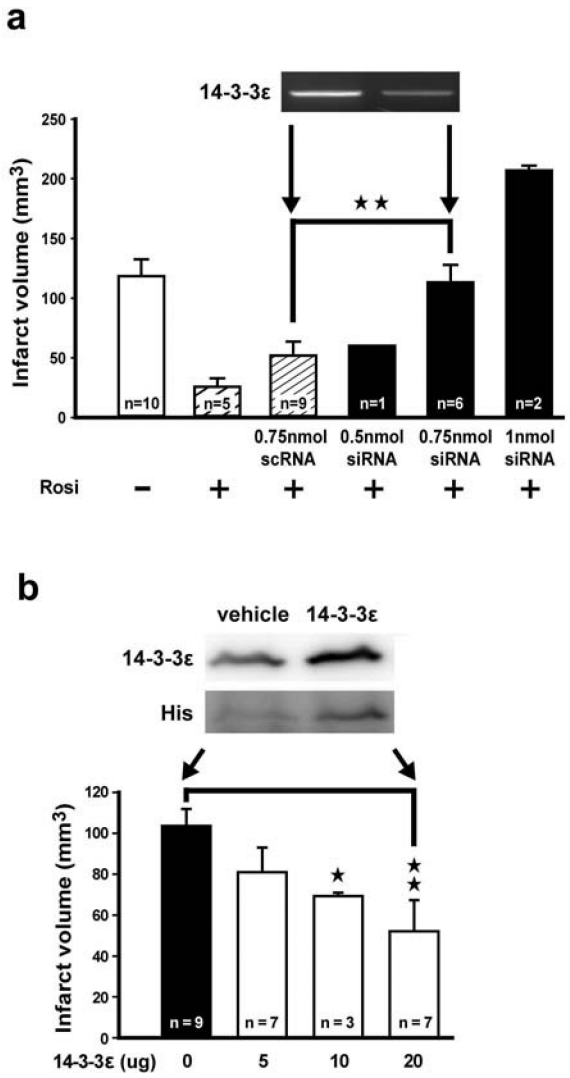

Figure 5. Control of cerebral infarction by 14-3-3ε *in vivo*

(a) Rosiglitazone with or without 14-3-3ε siRNA or scRNA was injected immediately after 30-min ischemia. Inset shows cortical 14-3-3ε mRNA levels. Similar results were obtained in two other experiments. **(b)** His-tagged 14-3-3ε recombinant proteins (5~20 μg) were infused 72 h before I/R. Inset shows 14-3-3ε and His analyzed by Western blotting. Each bar denotes mean ± SD. **P*<0.05. ***P*<0.01. Similar results were obtained in two other experiments.

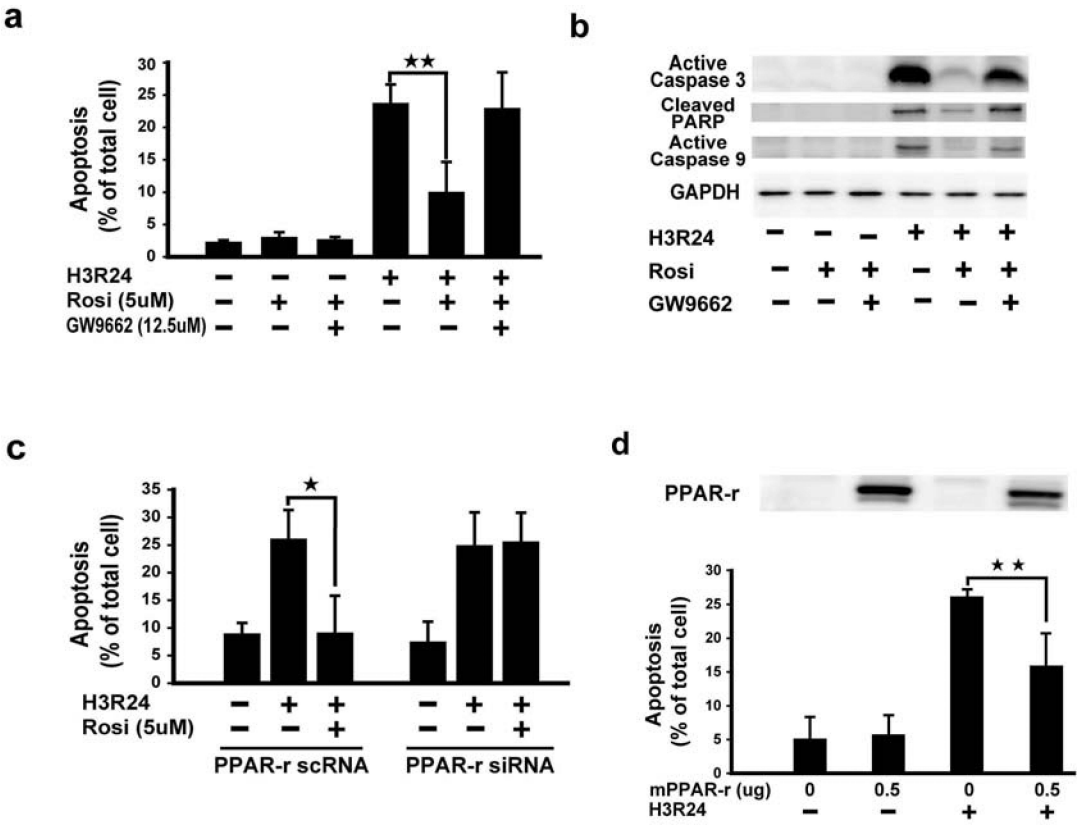

Figure 6. Rosiglitazone attenuates N2-A apoptosis in a PPAR-γ dependent manner

(a) Cells were subjected to OGD for 3h followed by reoxygenation for 24 h (H3R24) with or without rosiglitazone (Rosi) and/or GW9662. Apoptosis was analyzed by flow cytometry. **(b)** Cells were treated as **a)** and active caspase 3, 9 and cleaved PARP were determined by Western blotting. A representative blot is shown. **(c)** N2-A cells transfected with PPAR-γ siRNA or control were subjected to OGD (H3R24) with or without Rosi. **(d)** Cells transfected with PPAR-γ plasmids were subjected to H3R24. Upper panels show PPAR-γ proteins analyzed by Western blotting. Each bar denotes mean ± SD from at least three independent experiments conducted in triplicate. **P*<0.05. ***P*<0.01.

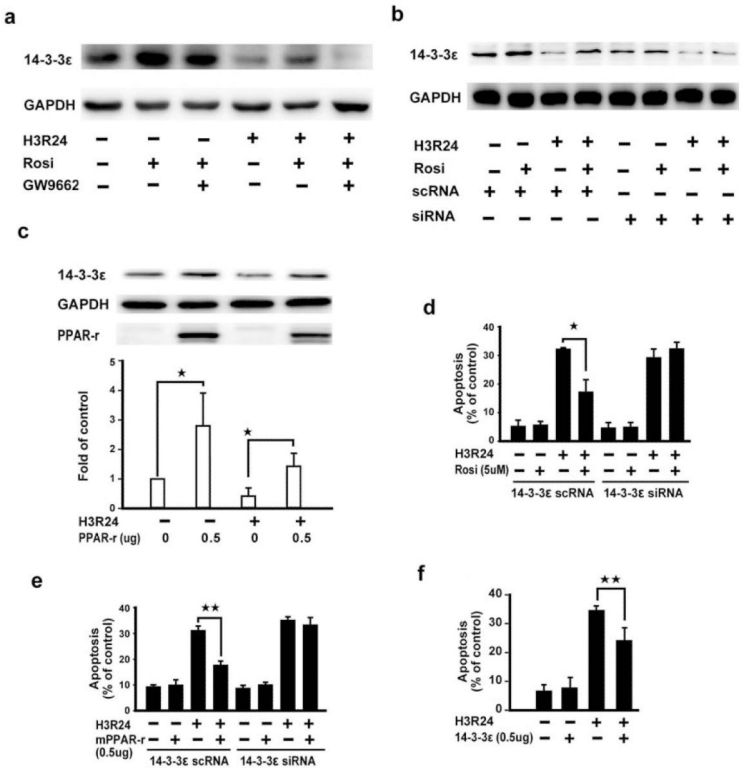

Figure 7. Rosiglitazone and PPAR-γ restore 14-3-3ε

(a) N2-A cells were subjected to OGD (H3R24) in the presence or absence Rosi and GW9662, and protein levels of 14-3-3ε were measured. **(b)** Cells transfected with PPAR-γ siRNA or control scRNA were subjected to H3R24 in the presence or absence of Rosi. **(c)** Cells transfected with PPAR-γ plasmids were subjected to H3R24. The upper panel shows a representative blot and the lower panel, the densitometry analysis. **(d) & (e)** Cells transfected with 14-3-3ε siRNA or control scRNA were subjected to H3R24 with or without Rosi **(d)** or PPAR-γ transfection **(e)**. **(f)** N2-A transfected with 14-3-3ε plasmids were subjected to H3R24. Each bar denotes mean ± SD of at least three independent experiments conducted in triplicate. **P*<0.05. ***P*<0.01.

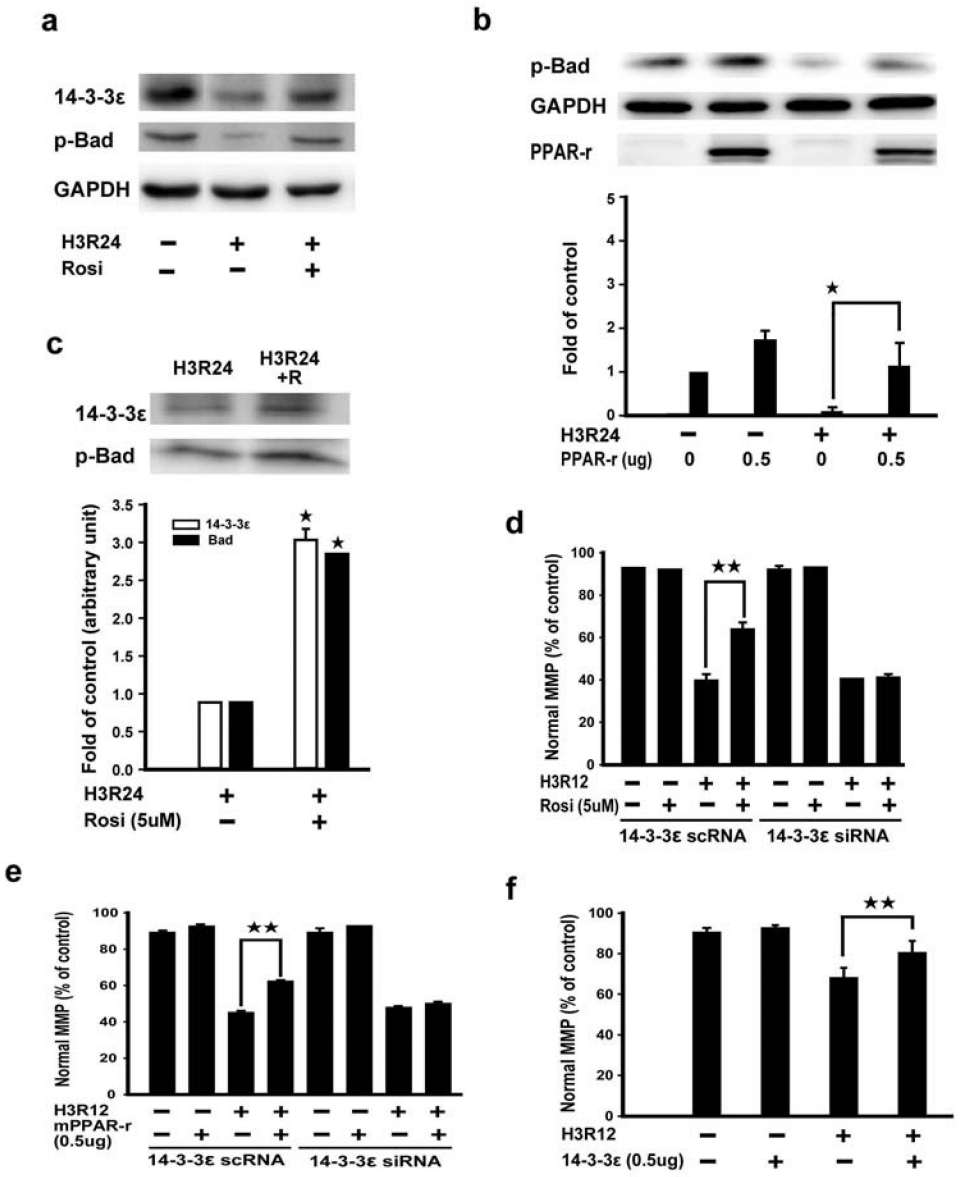

Figure 8. Interaction between 14-3-3ε and phosphorylated Bad (p-Bad)

(a) & (b) N2-A cells were subjected to H3R24 in the presence or absence of Rosi **(a)** or PPAR-γ **(b)**. 14-3-3ε and p-Bad were analyzed by Western blotting. **(c)** Cells treated with H3R24 in the presence or absence of Rosi (R) were lysed and immunoprecipitated with a 14-3-3ε antibody. Proteins in the immunoprecipitate were analyzed by Western blotting using p-Bad or 14-3-3ε antibodies. Upper panels show representative immunoblots and the lower panels densitometry analysis. **(d) & (e)** Cells were transfected with 14-3-3ε siRNA or control and subjected to H3R12 in the presence or absence of Rosi **(d)** or PPAR-γ **(e)**. MMP was analyzed by flow cytometry using JC-1 probe. **(f)** MMP was measured in cells treated with H3R12 in the presence or absence of 14-3-3ε plasmids. Each bar represents mean ± SD of at least three experiments. **P*<0.05. ***P*<0.01.